Molecular Crystals and Liquid Crystals

Publication details, including instructions for authors and subscription information:
http://www.tandfonline.com/loi/gmcl20

Comparison of Theoretical and Experimental switching curves for a zenithally bistable nematic liquid crystal device

C. V. Brown [a] , L. Parry-Jones [a] , S. J. Elston [a] & S. J. Wilkins [b]

[a] Department of Engineering Science, Oxford University, Oxford, United Kingdom

[b] Physical and Theoretical Chemistry Laboratory, Oxford University, Oxford, United Kingdom

Version of record first published: 18 Oct 2010

To cite this article: C. V. Brown, L. Parry-Jones, S. J. Elston & S. J. Wilkins (2004): Comparison of Theoretical and Experimental switching curves for a zenithally bistable nematic liquid crystal device, Molecular Crystals and Liquid Crystals, 410:1, 417-425

To link to this article: http://dx.doi.org/10.1080/15421400490433451

Mol. Cryst. Liq. Cryst., Vol. 410, pp. 417/[945]–425/[953], 2004

ISSN: 1542-1406 print/1563-5287 online
DOI: 10.1080/15421400490433451

Taylor & Francis
Taylor & Francis Group

COMPARISON OF THEORETICAL AND EXPERIMENTAL SWITCHING CURVES FOR A ZENITHALLY BISTABLE NEMATIC LIQUID CRYSTAL DEVICE

C. V. Brown, L. Parry-Jones, and S. J. Elston
Department of Engineering Science, Oxford University, Parks Road, Oxford OX1 3PJ, United Kingdom

S. J. Wilkins
Physical and Theoretical Chemistry Laboratory, Oxford University, South Parks Road, Oxford OX1 3QZ, United Kingdom

Zenithally bistable nematic liquid crystal devices have been fabricated from a interferometrically defined microgrooved surface and a flat substrate treated with homeotropic surfactant. Two stable states are observed in the devices, one where the liquid crystal is aligned homeotropically (VAN) and the other where the alignment is planar at the grooved surface (HAN). The time-voltage switching curves have been measured using an automated addressing and detection system for switching from HAN to VAN and viceversa. The values of the surface energy and the flexoelectric $e_{11} + e_{33}$ coefficient have been estimated by comparing these with theory.

Keywords: flexoelectricity; nematic liquid crystal; zenithal bistable device

1. INTRODUCTION

Bistable nematic LCDs combine many of the advantages of conventional twisted nematic displays with the additional ability to retain an image in the power-off state. Passive matrix addressed displays based on these switching modes would be rugged and have low power consumption. Such displays have a high potential for becoming the technology of choice for use

The authors gratefully acknowledge A. J. Davidson, N. J. Mottram and Dr. S. J. Sheard for useful discussions, Prof. R. G. Compton for access to the AFM facilities, and the EPSRC for funding.

Address correspondence to C. V. Brown, Department of Engineering Science, Oxford University, Parks Road Oxford, OX1 3PJ, United Kingdom. E-mail: Carl.brown@ntu.ac.uk

in high volume market application such as mobile phones, programmable smart-cards and camcorder viewfinders.

In Zenithally Bistable Nematic Devices (ZBND) there are two stable orientations of the nematic liquid crystal that have substantially different tilt angles [1–4]. The ZBND devices that have been studied here consists of a layer of nematic liquid crystal material that is sandwiched between a monograting surface and a flat surface. Both of these surfaces are coated with a homeotropic agent.

Two energetically stable alignment textures of the liquid crystal molecules in ZBND devices are depicted in Figure 1. In (1a) nematic defect occur near to the peaks and troughs of the grooves resulting in a hybrid alignment (HAN). In (1b) the shape of the elastic deformation follows the contours of the grating resulting in a homeotropic alignment profile (VAN). Switching between the HAN and VAN states has been achieved using monopolar pules of alternating polarity. The mechanism for switching to the VAN state is thought to be the usual interaction between the applied field and the dielectric anisotropy. For switching to the HAN state the coupling to the flexoelectric polarization is thought to play the dominant role [1,5]. The actual switching process is complicated because it involves domain motion and also the creation and annihilation of defects.

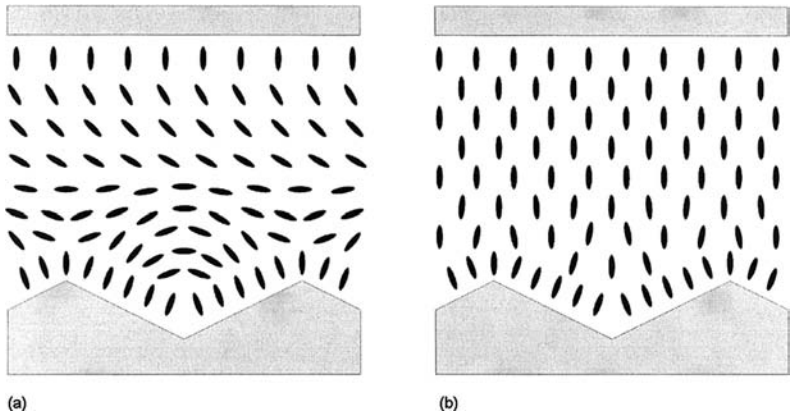

FIGURE 1 Stable nematic liquid crystal director configurations that occur for a nematic confined between a flat surface and a grooved surface that have both been treated with a homeotropic surfactant. (a) hybrid aligned state (VAN) and (b) homeotropic state (HAN).

2. GRATING FABRICATION AND CHARACTERISATION

The surface relief structures were fabricated using an interferometric exposure technique [6]. The substrates were pieces of glass of thickness 1.1 mm coated with indium tin oxide with a resistivety of less than 100 Ohms per square. The pre-cleaning process involved washing in Decon detergent solution, acetone, isopropylalcohol, and finally baking for 30 minutes at 125°C. After cooling the substrates were flooded with Shipley S1813 photoresist applied from a syringe through a 0.22 μm filter and then spun on a vacuum chuck for 30 seconds at 4200 r.p.m. The photoresist solvent was removed by furter baking for 30 minutes at 90°C.

A sinusolidal intensity pattern of period 1.0 μm was provided by the interference between two beams of light that had been derived from the same laser source [7] giving an average intensity at the sample of 5.0 mW/cm^2. After exposure for 6 seconds the surface relief pattern was developed by immersion in 1:1 Microposit developer to DI water for 90 seconds at 21°C. The photoresist layer was hardened by baking for 1 hour in a vacuum oven at 130°C, and by a long flood exposure to UV light in an EPROM eraser.

The surface grating profiles were characterized using an Atomic Force microscope [8]. This had been fitted with a conical probe of length 4 μm and half-angle 35° [9]. The maximum depth of a sinusoidal surface relief structure of pitch 1.0 μm that could be resolved with this probe was 350 nm. A typical AFM picture is shown in Figure 2 and, noting the maximum depth resolution, this has a roughly sinusoidal profile. It is clear

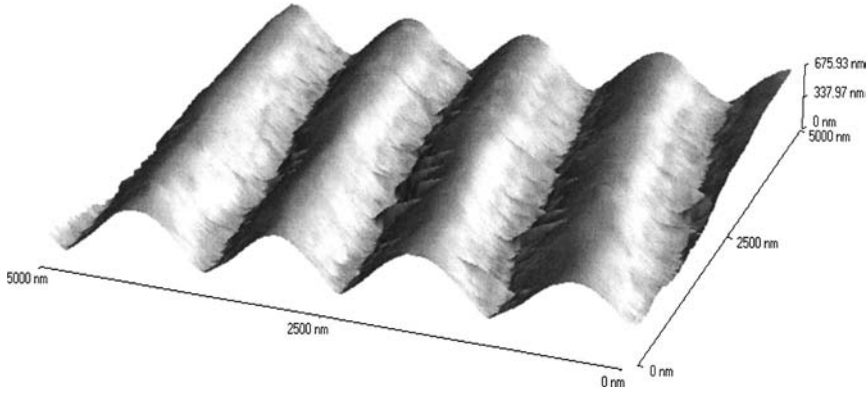

FIGURE 2 Typical surface relief grating profile measured using atomic force microscopy.

that the surface relief structure is defined within the width of the photoresist layer and there is no exposure through to the ITO substrate.

ZBND devices were assembled from a flat ITO/glass substrate and a substrate with a surface relief pattern. Both the substrates had been coated with a uni-molecular layer of chrome complex homeotropic alignment agent [10]. A 7 μm gap was created between the substrates using spacer beads suspended in UV activated adhesive. The cells were capillary filled in a vacuum with E7 nematic liquid crystal material in the isotopic phase. When the cells were first cooled a mixture of light and dark domains was spontaneously formed and domain widths varying from the size of a single grating prove to about 20–30 μm could be observed using a polarizing microscope.

3. EXPERIMENTAL MEASUREMENTS

Measurements have been made of the Voltage-Time switching curves of device in response to monopolar switching pulses. An automated addressing and detection system was used to generate the pulses and to map out the intensity change in response to pulses of varying durations and voltage amplitudes. The apparatus that was used is illustrated in Figure 3. The PC computer controlled a Wavetek 395 arbitrary function generator and read the values of the transmission levels before and after the pulses were applied from the oscilloscope. A microscope objective was used to focus

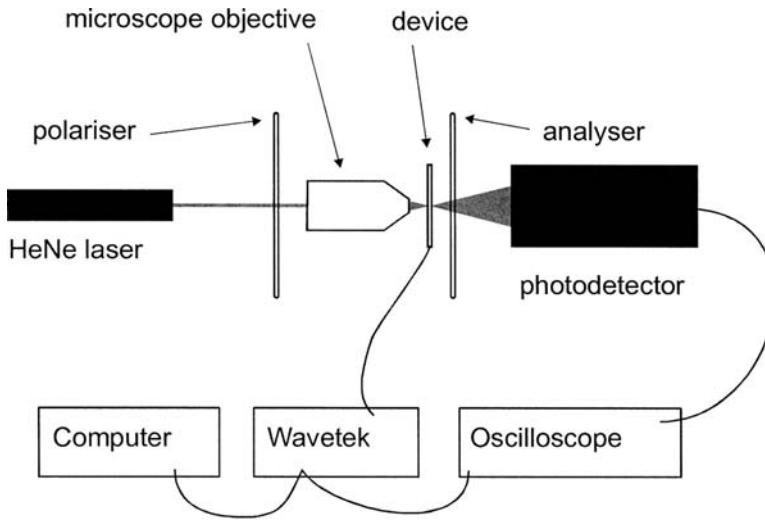

FIGURE 3 Automated measurement and data acquisition aparatus.

the laser light from the HeNe laser so that the switching curves correspond to an area of approximately 50 μm on the ZBND device. The polarisor and analyzer were crossed with the polarisor set at 45° to the lines of the grating. This gives the maximum optical contrast between the VAN and HAN states.

The experimental curves for room temperature switching from the VAN to the HAN state are shown in Figure 4a and for switching from the HAN to

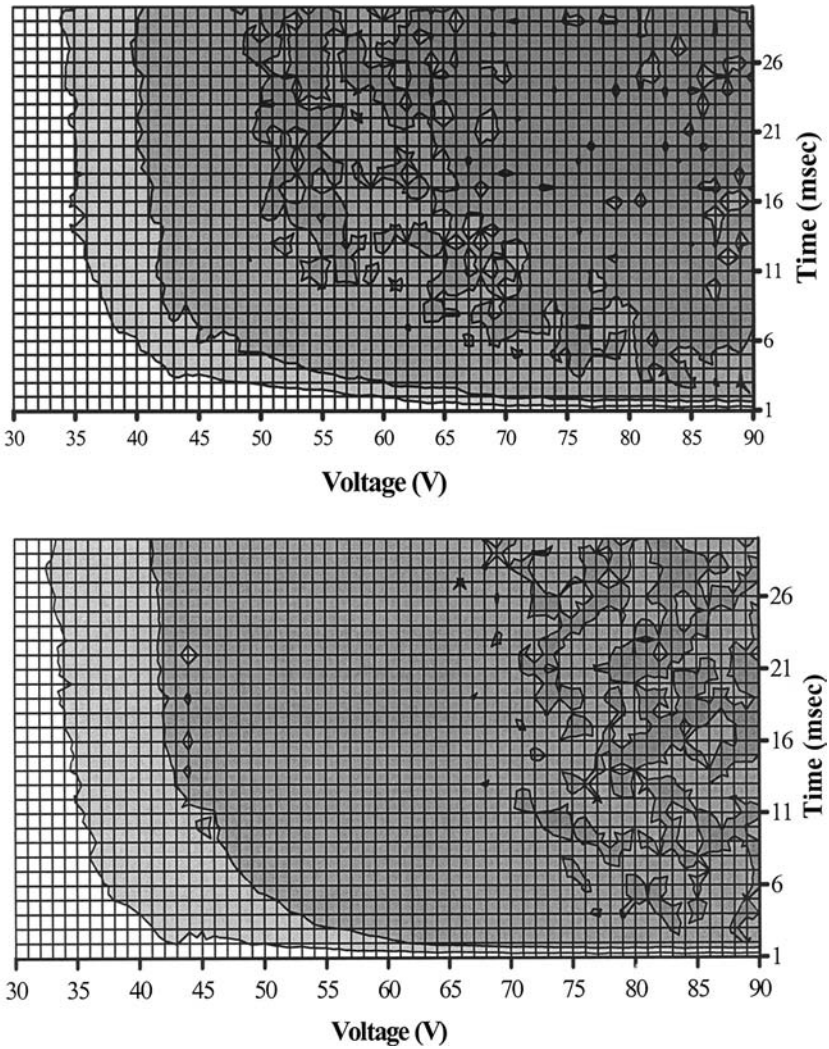

FIGURE 4 Experimental curves for switching (a) from the VAN state to the HAN state, and (b) from the HAN state to the VAN state.

the VAN in Figure 4b. In each case the initial state was stabilized by applying a blanking pulse of 20 msec duration and 80 Volt amplitude. A switching pulse was then applied and the averaged transmission level between 100 and 300 msec after the switching pulse was then measured using the photodiode. The graphs in Figure 4 are contour plots showing of the transmission level after the switching pulse normalized to the transmission of the state that is being switched into when it is relaxed in equilibrium. The line between the white area and the light grey area corresponds to 50% partial switching, and the line between the light and dark grey area to 75% partial switching.

4. ANALYSIS OF RESULTS

The shapes of the switching curves have been simulated using a 1-dimensional theoretical model that is similar to that presented in [11]. The nematic director $\boldsymbol{n}$ is written in terms of the Zenithal angle θ, i.e. $\boldsymbol{n}(z) = (\cos\theta(z), 0, sin\,\theta(z))$, where z is the distance between the bounding plates at $z = 0$ and $z = d$. Using this definition $\theta = 0$ corresponds to the director lying parallel to the bounding plates, and for $\theta = \pi/2$ the director lies perpendicular to the bounding plates. For the homeotropic alignment on the upper plate $\theta(z = d) = \pi/2$. On the lower plate the two states are described using a surface energy term of the Rapini–Papoular form [12] shown in Eq. (1) where $\theta_0 = \theta(z = 0)$. This gives surface energy minima at $\theta_0 = 0$ and $\theta_0 = \pi/2$.

$$W_s = \frac{W_0}{2}\sin^2(2\theta_0) \tag{1}$$

The time evolution of the nematic liquid crystal director orientation is calculated using nematic continuum theory in 1d, as shown in Eq. (2). Due to the balance of surface torques this is subject to the boundary condition shown in Eq. (3) at the surface $z = 0$.

The theory includes the coupling of the applied electric filed to the flexoelectric polarization.

$$\eta\left(\frac{\partial\theta}{\partial t}\right) = \frac{1}{2}(K_{11} - K_{33})\sin 2\theta\left(\frac{d\theta}{dz}\right)^2 - \left(K_{11}\cos^2\theta + K_{33}\sin^2\theta\right)\left(\frac{d^2\theta}{dz^2}\right) - \frac{1}{2}\varepsilon_0\Delta\varepsilon\sin 2\theta E_z^2 \tag{2}$$

$$\left(K_{11}\cos^2\theta + K_{33}\sin^2\theta\right)\left(\frac{d\theta}{dz}\right) + \frac{1}{2}e\sin 2\theta E_z + 2W_0\cos 2\theta\sin 2\theta = 0 \tag{3}$$

TABLE 1 Values of the Physical Parameters Used to Obtain the Theoretical Switching Curves

Description	Symbol	Value
Splay elastic constant	k_{11}	11.7 pN
Bend elastic constant	k_{22}	19.5 pN
Dielectric anisotropy	$\Delta\varepsilon$	19.5
Switching viscosity	η	$0.05\,\mathrm{Ns/m^2}$
Flexoelectric coefficient	e	$6.0 \times 10^{-10}\,\mathrm{Cm}$
Surface energy	W_0	$2.0 \times 10^{-5}\,\mathrm{Nm^{-1}}$

Here K_{11} and K_{33}, are the splay and bend elastic constants respectively, $\Delta\varepsilon$ is the dielectric anisotropy, η is the effective switching viscosity, and e is the flexoelectric coefficient $e = e_{11} + e_{33}$.

Equations (2) and (3) have been solved using a numerical relaxation method. It has been assumed that the electric field E_z is constant throughout the liquid crystal layer and is given by the ratio of the applied voltage V to the layer thickness d. Literature values of K_{11}, K_{33}, and $\Delta\varepsilon$ for the material E7 [13] have been used as constant in the model, these values are shown in (Table 1).

In Figure 5 theoretical curves are shown for switching from the VAN to the HAN state in (a) and for switching from the HAN to the VAN state in (b). The values of the flexoelectric coefficient $e = e_{11} + e_{33}$ and the effective surface energy W_0 were used as variables that were adjusted in order to obtain curves that resemble the experimental curves shown in Figure 5. The effective switching viscosity η was also allowed to vary in a limited range since a 1 d model is being used here to describe what is in essence a 2d/3d switching phenomenon involving the creation and annihilation of defects. It was found that the best description of the experimental curves for switching both from VAN to HAN and also from HAN to VAN was obtained for the values of e, W_0 and η shown in Table 1.

5. DISCUSSION AND CONCLUSIONS

The value for the surface energy is very similar to value obtained in similar devices from measurement and theoretical fitting of the diffracted intensities [14]. A flexoelectric coefficient of 6.0×10^{-10}Cm in the theoretical model gives the closest resemblance to the experimental data. This value is well over an order of magnitude higher than the value of 1.5×10^{-11} Cm that has been reported in the literature from the fitting of accurately determined hybrid director profiles in hybrid cells [15]. The theoretical curves do not

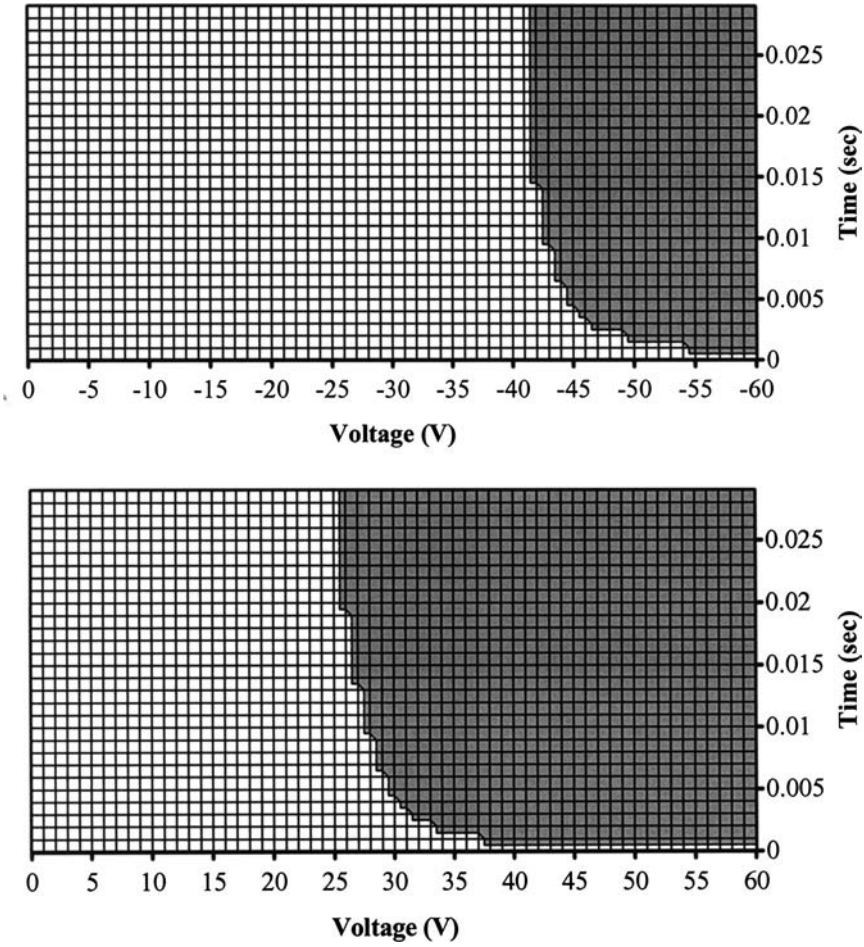

FIGURE 5 Theoretical curves for switching (a) from the VAN state to the HAN state, and (b) from the HAN state to the VAN state.

reproduce the experimental data well. The main difference between the two is that experimentally the VAN to HAN and HAN to VAN curves have similar "threshold" voltages below which only 25% partial switching occurs. For the model that was used these thresholds differed by 15 Volts. There are many reasons for the difference between the theory and the experiment.

Here a simplified 1d model has been used in order to fit the switching reponse for what is essentially a nucleated domain switching process in 2 and 3d involving complicated dynamic flow. The 1 d model may be appropriate to describe the first nucleation point in the switching process before

domain evolution occurs – a similar approach has been taken to modelling surface stabilised ferroelectric liquid crystal devices [16]. An additional simplification in the approach taken here is the choice of the Rapini–Papoular from for the surface energy in Eq. (1). Work is underway to develop more physically realistic forms of surface energy by making use of theoretically generated models of the 2d director profiles similar to the illustration in Figure 1 [17].

Future work will atempt to relate the shapes of the experimental switching curves to the geometry of the surface profile. This will require more accurate determination of the grating profile using an AFM machine fitted with a high aspect ration probe tip. It is also intended to generate different surface profile shapes using hard contact photolithography with both on-axis and off-axis illumination.

REFERENCES

[1] Bryan-Brown, G. P., Brown, C. V., & Jones, J. C. (1997). Patent numbers GB232318422A, EP0856164A. Bryan-Brown, G. P., Brown, C. V., Jones, J. C., Wood, E. L., Sage, I. C., Brett, P., & Rudin, J. SID digest, vol. XXVIII, 37–40.
[2] Boyd, G. D., Cheng, J., & Ngo, P. D. T. (1980). *Appl. Phys. Lett.*, *36*, 556.
[3] Cheng, J., Thurston, R. N., Boyd, G. D., & Meyer, R. B. (1982). *Appl. Phys. Lett.*, *40*, 1007.
[4] Guyon, E., Pieranski, P., & Boix, M. (1984). *Lett. Appl. Eng. Sci.*, *1*, 19.
[5] Barberi, R., Giocondo, M., & Durand, G. (1992). *Appl. phys. Lett.*, *60*, 1085.
[6] Hutley, M. C. (1982). *Diffraction Gratings*, Academic Press: London.
[7] 442 nm spectral line, Helium-Cadmium laser, Kimmon IK412IR-G.
[8] EasyScan AFM system, Nanosurf A.G.
[9] General purpose contact mode SiN cantilever, ThermoMicroscopes.
[10] Matsumoto, S., Kawamoto, M., & Kaneko, N. (1975). *Appl. phys. Lett.*, *27*, 268.
[11] Davidson, A. J. & Mottram, N. J. (2002). *phys. Rev. E*, *65*, 051710.
[12] Rapini, A. & Papoular, M. (1969). *J. Physique Colleq.*, *30*, C4–54.
[13] Berreman, D. W. (1972). *Phys. Rev. Lett.*, *28*, 1683.
[14] Edwards, E. G. *et al.* submitted to *Mol. Cryst. Liq. Cryst.* proc. ILCC 2002
[15] Jewell, S. A. & Sambles, J. R. (2002). *J. Appl. Phys.*, *92*, 19.
[16] Maclennan, J. E. (1988). Ph.D. thesis, University of Boulder, Colorado.
[17] Parry-Jones, L., Edwards, E. G., Elston, S. J., & Brown, C. V. (2003). submitted to *App. Phys. Lett.*, *82*, 1476.